
Article:
Wills, C.R., Malandrino, A., Van Rijsbergen, M. et al. (3 more authors) (2016) Simulating the sensitivity of cell nutritive environment to composition changes within the intervertebral disc. Journal of the Mechanics and Physics of Solids, 90. pp. 108-123. ISSN 0022-5096

https://doi.org/10.1016/j.jmps.2016.02.003

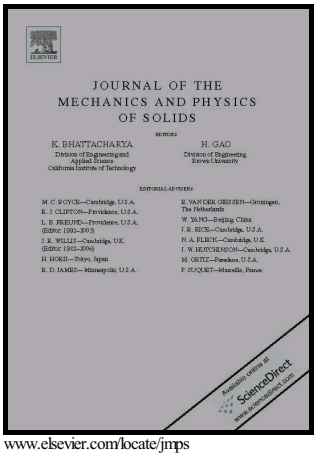

www.elsevier.com/locate/jmps

Simulating the sensitivity of cell nutritive environment to composition changes within the intervertebral disc

C. Ruiz Wills, A. Malandrino, MM. van Rijsbergen, D. Lacroix, K. Ito, J. Noailly

PII: S0022-5096(16)30090-4
DOI: http://dx.doi.org/10.1016/j.jmps.2016.02.003
Reference: MPS2792

To appear in: *Journal of the Mechanics and Physics of Solids*

Received date: 5 December 2014
Revised date: 27 November 2015
Accepted date: 6 February 2016

Cite this article as: C. Ruiz Wills, A. Malandrino, MM. van Rijsbergen, D Lacroix, K. Ito and J. Noailly, Simulating the sensitivity of cell nutritiv environment to composition changes within the intervertebral disc, *Journal of th Mechanics and Physics of Solids,* http://dx.doi.org/10.1016/j.jmps.2016.02.003

Simulating the sensitivity of cell nutritive environment to composition changes within the intervertebral disc

C. Ruiz Wills[1,2], A. Malandrino[2], MM. van Rijsbergen[3], D. Lacroix[4], K. Ito[3], J. Noailly[1,2*]

[1]Department of Communication and information Technologies (DTIC), Universitat Pompeu Fabra (UPF), Barcelona, Spain

[2]Biomechanics and Mechanobiology, Institute for Bioengineering of Catalonia (IBEC), Barcelona, Spain

[3]Department of Biomedical Engineering, Eindhoven University of Technology, Eindhoven, The Netherlands

[4]INSIGNEO Institute for In Silico Medicine, Department of Mechanical Engineering, University of Sheffield, Sheffield, UK

*Corresponding author.
jerome.noailly@upf.edu (J. Noailly)
Postal address: C/ Roc Boronat, 138, 08018 Barcelona, Spain
Tel. +34 93 542 15 79

Abstract

Altered nutrition in the intervertebral disc affects cell viability and can generate catabolic cascades contributing to extracellular matrix (ECM) degradation. Such degradation is expected to affect couplings between disc mechanics and nutrition, contributing to accelerate degenerative processes. However, the relation of ECM changes to major biophysical events within the loaded disc remains unclear. A L4-L5 disc finite element model including the nucleus (NP), annulus (AF) and endplates was used and coupled to a transport-cell viability model. Solute concentrations and cell viability were evaluated along the mid-sagittal plane path. A design of experiment (DOE) was performed. DOE parameters corresponded to AF and NP biochemical tissue measurements in discs with different degeneration grades. Cell viability was not affected by any parameter combinations defined. Nonetheless, the initial water content was the parameter that affected the most the solute contents, especially glucose. Calculations showed that altered NP composition could negatively affect AF cell nutrition. Results suggested that AF and NP tissue degeneration are not critical to nutrition-related cell viability at early-stage of disc degeneration. However, small ECM degenerative changes may alter significantly disc nutrition under mechanical loads. Coupling disc mechano-transport simulations and enzyme expression studies could allow identifying spatiotemporal sequences related to tissue catabolism.

Key terms: Intervertebral disc degeneration, Tissue composition, Finite element analysis, Cell nutrition, Multiphysics.

1. Introduction

Low back pain is a common clinical problem, in many cases related to the degeneration of the intervertebral disc (IVD) (Battié et al. 2007). The disc is a cartilaginous structure composed by four distinct regions. The outer ring is the annulus fibrosus (AF), a fibrous cartilage that surrounds a gelatinous core called the nucleus pulposus (NP). A transition zone (TZ) bridges these two regions, and a thin layer of hyaline cartilage, i.e. the cartilage endplates (CEP), separates the NP and TZ from the bone (Guilak et al. 1999; Roberts and Urban 2011). All sub-tissues are structurally and mechanically different but also highly bounded to each other, contributing to the functional mechanics of the IVD.

The mechanical and biophysical functionalities of the disc are determined by both the biochemistry and the ultrastructure of the extracellular matrix (ECM) (Setton and Chen 2004). The NP has a high concentration of negatively charged proteoglycans. On one hand, these proteoglycans lead to tissue swelling, which stretches the fibres of the surrounding AF. Both the mechanical resistance of the latter and the pressurization of the interstitial fluid of the NP provide the IVD with a unique balance of flexibility and mechanical strength (Setton and Chen 2004). On the other hand, the concentration of proteoglycans in the NP affects the rate at which molecules can diffuse through the tissue (Urban et al. 2004), while it also depends on disc deformations. More generally, the disc ECM, i.e. a collagen network embedded in a dense proteoglycan gel, acts as a selective physical barrier to the diffusion of molecules into the disc and controls the diffusive exchange of molecules with the surrounding tissues.

The IVD has a very low density of cells in comparison to other tissues; only 1% of the disc volume is occupied by cells (Roberts and Urban 2011). Nevertheless the continuing activity of cells largely controls the fate of the disc. On one hand, cells produce the macromolecules that keep the disc tissues functional with the passage of time (Roberts and Urban 2011). On the other hand, they are able to trigger catabolic processes that may accelerate the depletion of ECM components. The ECM balance that results from these processes affects directly the biomechanical function of the intervertebral disc as well as numerous biochemical processes.

In particular, essential solutes such as oxygen and glucose are supplied to the IVD from the blood vessels located at the margins of the organ (Urban et al. 2004). The further transport of these solutes to the cells relies mainly on diffusion within the fluid phase that saturates the disc ECM (Urban et al. 2004). Disc cells consume oxygen and glucose and produce lactic acid (glycolysis). While the lack of glucose can be a strong trigger of catabolic cell responses (Neidlinger-Wilke et al. 2012), the lack of oxygen was reported to alter the proteoglycan production (Horner and Urban 2001). At the same time, acid lactic needs to be removed in order to avoid any drop of pH in the extracellular medium. The local balance of these important chemical entities is governed by the properties of both the ECM and the solutes (Urban et al. 2004).

In the mechanically loaded IVD, it is intuitive to anticipate that tissue compaction, i.e. consolidation, and the resulting changes in both diffusion distances and fluid fractions affect solute diffusion. With disc degeneration, proteoglycan depletion is the most important biochemical change, and because of the consequent a fall in the osmotic pressure, the disc becomes less able to maintain hydration when loaded mechanically (Urban and Roberts 2003). Tissue fibrosis might happen concurrently, contributing to increase the relative amount of solid phase at the detriment of the fluid phase. Addressing the difficulty to explore experimentally the effect of these alterations on disc cell nutrition at the organ level, different finite element (FE) studies have been proposed.

Malandrino et al. (2011) studied the coupling between disc poromechanics and metabolic transport. They found that mechanical loads and tissue properties might affect significantly the distribution of oxygen and lactate when large and prolonged volume changes are involved. Also, the simulation results obtained by Galbusera et al. (2011) suggest that water loss inside the disc can induce cell death because of a reduced diffusion of nutrient and waste products. For a given disc geometry, a predominant impact of tissue consolidation on nutrition-related cell death was further reported based on the calculations results obtained by Malandrino et al. (2014a). Interestingly, Zhu et al. (2012) found that dynamic compression might limit nutrition-related cell death when degenerated disc properties were simulated, whilst earlier reported simulations suggested that dynamic loads limit the mechanically-induced water loss from the disc (Ruiz et al. 2013). However, none of the reported mechano-transport models

incorporated explicit information about ECM composition, e.g. proteoglycan, collagen and water content, and the precise influence of ECM composition changes on IVD cell viability remains unaddressed.

In order to clarify the relationships between ECM composition, disc degeneration, nutrition, and cell viability, a comprehensive analysis is needed with explicit consideration of degeneration-dependent changes in proteoglycan, collagen and water. Schroeder et al. (2007) have reported an osmoporoviscoelastic constitutive model for the AF and NP disc tissues, the parameters of which depended on the biochemical composition and organization of these tissues. For the first time, such a model allowed describing the internal mechanical conditions of the disc as a function of assessable ECM characteristics, through the FE method.

Accordingly, the present study aimed to combine the respective assets of mechano-transport simulations and composition-based tissue modelling in the IVD, in order to study how degenerative changes in disc composition may affect cell nutrition under mechanical loads. The biochemical changes explored were based on previous measurements of collagen, proteoglycan and water contents in healthy and mildly-moderately (Pfirrmann grade 3) degenerated discs. Numerical explorations were based on a systematic parametric analysis of the variation of these composition parameters, and metabolic transport results were extrapolated to the possible occurrence of nutrition-induced cell death.

2. Materials and methods

2.1. Disc model

A L4-L5 IVD model including the NP, the AF, the TZ and the CEP was used (Fig. 1) (Ruiz et al. 2013). For the NP, the TZ, and the AF, tissue constitutive models described the poromechanical interactions between: a hyperelastic porous matrix, saturated by intra and extra-fibrillar fluid, a swelling pressure stress simulated the Donnan osmotic effects, and viscoelastic collagen fibres (AF only) (Roberts and Urban 2011; Schroeder et al. 2007). The total stress tensor, $\boldsymbol{\sigma}$, was given by the sum of a pore pressure component p and the effective stress of the porous solid skeleton, $\boldsymbol{\sigma_{eff}}$:

$$\boldsymbol{\sigma} = \boldsymbol{\sigma_{eff}} - p\boldsymbol{I} \quad (1)$$

where **I** is the identity tensor and where the pore pressure, p, is the sum of the water chemical potential, u_w, and a swelling pressure term $\Delta\pi$ (Schroeder et al. 2007):

$$p = u_w + \Delta\pi \quad (2)$$

The macroscopic stress-strain response of the solid matrix was controlled by an initial shear modulus (G_m), an initial solid fraction ($n_{s,0}$) and by the current deformation of the homogenised poroeleastic continuum. A modified neo-Hookean model was used to describe the finite strain behaviour of the material (Schroeder et al. 2007):

$$\boldsymbol{\sigma_{eff}} = -\frac{1}{6}\frac{Ln(J)}{J} G_m \boldsymbol{I}\left[-1 + \frac{3(J+n_{s,0})}{(-J+n_{s,0})} + \frac{3JLn(J)n_{s,0}}{(-J+n_{s,0})^2}\right] + \frac{G_m}{J}\left(\boldsymbol{B} - J^{2/3}\boldsymbol{I}\right) \quad (3)$$

where J is the determinant of the deformation gradient tensor **F**, **I** is the first invariant the left Cauchy-Green strain tensor **B**.

In (2), u_w was related to the velocity of the interstitial fluid through the permeability, by applying Darcy's law. As for the osmotic pressure gradient $\Delta\pi$, it was given by the expression (Schroeder et al. 2007):

$$\Delta\pi = \phi_{int} RT\left(\sqrt{c_{F,exf}^2 + 4\left(\frac{\gamma_{ext}^{\pm}}{\gamma_{int}^{\pm}}\right)^2 c_{ext}^2}\right) - 2\phi_{ext} RT c_{ext} \quad (4)$$

where ϕ_{int} and ϕ_{ext} are the internal and external osmotic coefficients respectively, γ_{int} and γ_{ext} are the internal and external activity coefficients, c_{ext} is the external concentration of salt and $c_{F,exf}$ is the proteoglycan fixed charge density that depends on both the extra-fibrillar water (n_{exf}) and the normal fixed charge density in mEq per millilitre of the total fluid (c_F), according to the expression:

$$c_{F,exf} = \frac{n_f c_F}{n_{exf}} \quad (5)$$

with,

$$n_{exf} = n_f - \varphi_{ci}\rho_{c,tot} \quad (6)$$

where n_f is the total fraction of water, φ_{ci} is a parameter that defines the intrafibrillar water per collagen mass, and $\rho_{c,tot}$ is the collagen content respect to the total wet weight. The hydraulic permeability of the tissue (κ) was expressed as (Schroeder et al. 2007):

$$\kappa = \alpha\left(1 - n_{exf}\right)^{-M} \quad (7)$$

where α stands for an initial permeability at zero strain, and M is a positive constant.

The collagen fibres in the AF were considered to have a unidirectional viscoelastic mechanical response, simulated by a Zener rheological model that was modified to account for finite strains through two nonlinear springs (Schroeder et al. 2007).

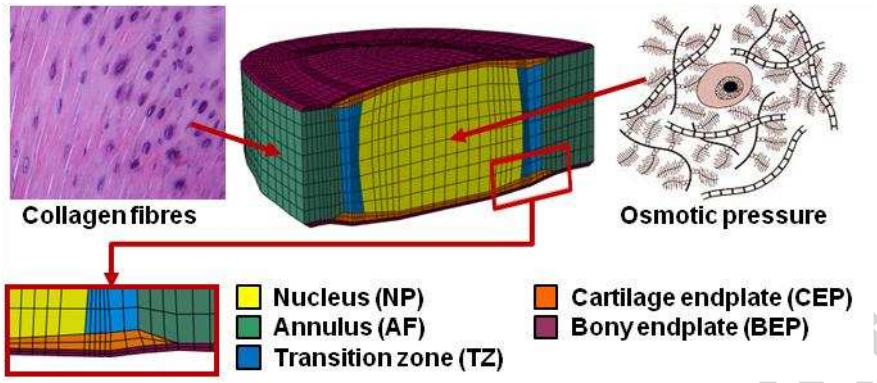

Fig.1 L4-L5 finite element disc model with all sub-tissues: nucleus pulposus (NP), annulus fibrosus (AF), transition zone (TZ), cartilage endplates (CEP) and bony endplates (BEP). Donnan osmotic pressure is included at the nucleus and the collagen fibres reinforcement in the annulus.

2.2. Tissue model parameters and relation to composition measurements

The tissue composition data from the literature (Urban & Maroudas 1979; Lyons et al. 1981; Urban and Holm 1986; Antoniou et al. 1996; Johannessen & Elliott 2005) were pooled and used in this study. They were obtained from IVD tissue samples through state-of-the-art experimental protocols and calculations that we briefly describe herein for the reader's information. To determine the water content, the wet weight (WW) of the tissue sample is measured first. Then, the sample is lyophilized and re-weighted to determine dry weight (DW), and the initial total water content (FF), from which $n_{s,0}$ (Eq. 3) and n_f (Eq. 5) are calculated, is determined according to:

$$FF = \frac{WW-DW}{WW} \quad (8)$$

$$n_{s,0} = 1 - FF \quad (9)$$

$$n_f = \frac{FF-1+J}{J} \quad (10)$$

where J is the determinant of the deformation tensor **F**

As for the estimation of the proteoglycan and total collagen content, the dried samples are digested in papain solution. Digested solutions are then used (i) to determine the content of sulfated Glycosaminoglycans (sGAG) through Dimethyl Methylene Blue (DMMB) assay (Farndale et al., 1986), and (ii) to achieve a measure for collagen content according to Hydroxyproline measurements, through the Chloramin-T assay (Huszar et al., 1980),

The initial fixed charge density $(c_{F,0})$ per per total hydrated tissue volume, from which c_F (Eq. 5) is calculated, was calculated by using the expression (Narmoneva et al. 1999):

$$c_{F,0} = \frac{z_{cs} c_{cs}}{MW_{cs}} \qquad (11)$$

$$c_F = c_{F,0} \frac{n_{F,0}}{n_{F,0} - 1 + J} \qquad (12)$$

where z_{cs}, MW_{cs}, and $c_{cs}$are the valency (2 mEq/mmol), the molecular weight (513000 μg/mmol), and the concentration (in μg/mL) of chondroitin sulfate, respectively, and $n_{F,0}$ is the intial water content. The sGAG content measured through the DMMB assay is assumed to be equivalent to the chondroitin sulfate content, i.e. c_{cs} is the amount of sGAG divided by the water content of the sample. To obtain $\rho_{c,tot}$ in Eq. (6), the initial collagen content (μg/mg DW) was estimated from hydroxyproline content by using 7.6 as the mass ratio of collagen to hydroxyproline (Sivan et al., 2006):

$$\rho_{c,tot} = \%\, hydroxyproline * 7.6 \qquad (13)$$

The stiffness constants and permeability were obtained in a previous study through numerical fits of model predictions to experimental measurements (Schroeder et al. 2008). Confined compression experiments were used to define the shear modulus G_m (NP: G_m = 1 MPa; AF: G_m = 0.84 MPa), the positive constant M (= 1.2), and the positive material constant α (= 0.00015 mm^4/Ns) of the tissue ground substance. Uniaxial tensile tests on annulus samples were used for the parameters of the reinforcing annulus fibres.

2.3. Transport and cell viability model

The composition-based disc model was coupled to a solute transport model according to a sequential workflow proposed by (Malandrino et al. 2011; 2014a). On

one hand, the solute transport considered the diffusion-reaction of oxygen, lactate and glucose:

$$\frac{\partial}{\partial t}\begin{pmatrix} C_{O_2} \\ C_{lact} \\ C_{gluc} \end{pmatrix} - \begin{pmatrix} D_{O_2} & 0 & 0 \\ 0 & D_{lact} & 0 \\ 0 & 0 & D_{gluc} \end{pmatrix} \nabla^2 \begin{pmatrix} C_{O_2} \\ C_{lact} \\ C_{gluc} \end{pmatrix} = \begin{pmatrix} R_{O_2} \\ R_{lact} \\ R_{gluc} \end{pmatrix} \quad (14)$$

where C_i, D_i and R_i are the concentrations, tissue diffusion coefficients, and the reactions of oxygen ($i = O_2$), lactate ($i = lact$) and glucose ($i = gluc$) respectively.

On the other hand, tissue deformations and interstitial fluid flow were linked to the reactive transport of these solutes through integration of the mechanically induced changes in porosity, as calculated through the poromechanical equations. Moreover, the effective diffusivity of each solute in the tissue (D_{solute}) was related to the solute diffusivity in water (D_{water}), according to the Mackie Meares model (Mackie and Meares 1955):

$$\boldsymbol{D}_{solute} = \frac{D_{water}\boldsymbol{I}}{(\theta)^2} \quad (15)$$

where θ is the total distance travelled by the solutes relative to a reference distance between two planes of a cubic lattice defined by the molecules of the solid phase. Comparing ions/metabolites diffusion in a porous membrane to diffusion in a liquid, e.g. water, θ was reported to scale as (Mackie and Meares 1955):

$$\theta = \frac{(1+n_s)}{(1-n_s)} \quad (16)$$

where n_s is the solid fraction of the matrix, that can be expressed in terms of the water content (n_f):

$$n_s = 1 - n_f \quad (17)$$

Replacing Eq. 17 in Eq. 16, we obtained:

$$\theta = \frac{(2-n_f)}{n_f} \quad (18)$$

And replacing Eq. 18 in Eq. 15 led to the expression:

$$\boldsymbol{D}_{solute} = \left(\frac{n_f}{2-n_f}\right)^2 D_{water}\boldsymbol{I} \quad (19)$$

As for the metabolic reactions, the model included the system of reactions reported by (Bibby et al. 2005):

- Oxygen cell consumption

$$R_{O_2} = -n_f \frac{7.28\rho_{cell,}}{S_{O_2}} \left(\frac{C_{O_2}(pH - 4.95)}{1.46 + C_{O_2} + 4.03(pH - 4.95)} \right) \quad (20)$$

- Lactate production

$$R_{lact} = \rho_{cell} exp\left[-2.47 + 0.93pH + 0.16C_{O_2} - 0.0058\left(C_{O_2}\right)^2 \right] \quad (21)$$

- Glucose consumption

$$R_{gluc} = -\frac{1}{2} R_{lact} \quad (22)$$

where R_{O_2} is in kPa/h, R_{lact} is in nmol/(mLh), R_{gluc} is in nmol/(mLh) , ρ_{cell} is the cell density of the tissue, $C_{O_2}$is the oxygen concentration in kPa. The pH was linked to the lactate concentration, C_{lact} (in nmol/mL), by the expression (Bibby et al. 2005):

$$pH = 7.4 + A \cdot C_{lact} \quad (23)$$

which is a linearization of experimental results of pH decay with lactate accumulation (Bibby et al. 2005), and 1/A = - 11.11 nmol/mL is a constant that quantifies change of pH per unit of lactate concentration.

The cell viability was considered as the ratio $\rho_{cell}/\rho_{cell,0}$, being the initial cell density $\rho_{cell,0}$ before any cell death occurs with tissue-specific values taken from the literature (Malandrino et al. 2011) (Table 1). Cell density change over time was based on the experimental study of Horner and Urban (2001), where 1 millions/mL cells in wells start to die exponentially without glucose and when the pH is acid. Thereby, the cell density was given by this expression:

$$\rho_{cell} = \rho_{cell,0} \exp(-\alpha_i t) \quad (24)$$

where the death rate for pH (α_{pH}) is constant and equal to $3.43x10^{-6}\ s^{-1}$, and the rate for glucose (α_{gluc}) is $9.28x10^{-6}\ s^{-1}$. These constants were directly derived by curve fitting, from the experiment of cells performed by Horner and Urban (2001) and ensured

an accurate representation of the spatiotemporal cell death patterns for cell density values relevant to the IVD, i.e. $4x10^6$ cells/mL and $8\ x10^6$ cells/mL (Malandrino et al. 2014b). The viability criteria were taken from previous studies (Horner and Urban 2001) where exponential decays start when: a) the glucose concentration decreases below 0.5 nmol/mL, b) the pH value is below 6.8 and c) both glucose and pH are below their critical values.

2.4. Boundary conditions

A day cycle of 8 hours of rest under 150 N compressive load and 16 hours of activity under 800 N in compression was repeated for three days (Wilke et al. 1999). The load was applied at the upper bony endplate while the lower bony endplate was fixed. External pressure was nil. Oxygen, lactate and glucose concentrations were applied at the outer surfaces of the CEP and of the AF (Fig.2a), and literature-based values (Malandrino et al. 2011) were used (Table 1). Before simulating the effect of any mechanical load, we initialized the transport model in other to achieve steady state solute concentrations throughout the IVD model. Transport parameters and cell viability were evaluated along the mid sagittal plane path: NP centre, anterior and posterior AF (Fig. 2b).

Table 1 Transport-cell viability parameters applied: oxygen concentration (C_{O_2}), lactate concentration (C_{lact}), glucose concentration (C_{gluc}) and cell density (ρ_{cell}).

Tissue	Boundary conditions at the edge			Initial condition
	C_{O_2} (kPa)	C_{lact} (nmol/mL)	C_{gluc} (nmol/mL)	ρ_{cell} (10^6 cells mm^{-3})
CEP	5.1	0.8	4	0.0135
AF	5.8	0.9	5	0.00555

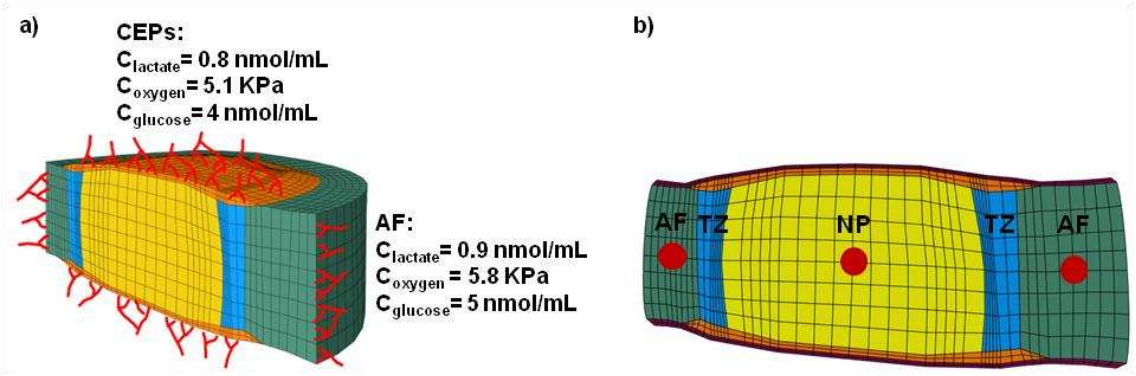

Fig.2 a) Solute boundary conditions applied at the surfaces of the annulus (AF) and cartilage endplates (CEPs) and b) Points selected for nutrition-cell viability evaluation: posterior annulus centre (left side), nucleus centre and anterior annulus centre (right side).

2.5. Design of experiment

A design of experiment (DOE) using a fractional factorial statistical method was performed, and variations were defined for the following biochemical parameters of the composition-based AF and NP models (Eqs. 4, 5 and 6): initial water content (n_{F0}), initial fixed charge density (c_{F0}) and collagen content ($\rho_{c,tot}$) (Table 2). For each parameter, variations in the DOE consisted in a switch between an upper level and a lower level parameter value. While upper level values corresponded to the composition data measured for Thompson grade I IVDs, lower level values corresponded to grade III IVDs (Thompson et al. 1990).

Table 2 Design of experiment parameters and values: annulus initial water content (n_{F0} AF), annulus collagen content ($\rho_{c,tot}$ AF), nucleus initial water content (n_{F0} NP), nucleus initial fixed charge density (c_{F0} NP) and nucleus collagen content ($\rho_{c,tot}$ NP).

Level	n_{F0} AF (*)	$\rho_{c,tot}$ AF (**)	n_{F0} NP (*)	c_{F0} NP (mEq/mL)	$\rho_{c,tot}$ NP (**)
Grade I	0.75	0.65	0.80	0.30	0.150
Grade III	0.70	0.78	0.76	0.23	0.285

* Fraction of wet weight ** Fraction of dry weight

A fractional factorial analysis of $2^{5-1} = 16$ runs was used, representing a resolution V. In fractional factorial designs, such a resolution allows thorough

identification of the main effects, without any confusion with multiple factor interactions. The significance of each parameter effect was analyzed statistically (Minitab Inc.) using an analysis of variance (ANOVA) with a significance threshold $\alpha = 0.05$. The standardized effect T_1 was calculated using the following equation:

$$T_1 = \frac{COEFF_1}{COEFF_{SE}} \tag{25}$$

where $COEFF_1$ is the effect coefficient of the parameter and $COEFF_{SE}$ is the standard error of the coefficient.

2.5. Convergence analysis and model validation under creep

The mesh convergence of the model was verified based on a comprehensive convergence study performed for the mesh template of the IVD model, including assessment of the stability of the poromechanical predictions (Ruiz et al. 2013). However, the transport model was sensitive to the time step selected for the calculations. As such, an additional convergence study was performed for the time discretisation of the transport model, so as to obtain the best compromise between accuracy of the results and computational cost at the different time points selected for the DOE. In order to validate the composition-based model under compression, the disc height reductions achieved after creep were compared to those reported in the literature after the experimental boundary conditions were simulated.

3. Results

The range solute concentrations obtained after the initialization of the transport model at nucleus were: 2.3-4.5 kPa for oxygen, 1.3-3.2 nmol/mL for lactate and 2.5-3.7 nmol/mL for glucose. After 900 s of creep under 500 N compressive load, a disc height reduction of 1.27 mm was calculated with the material properties representative of a grade I IVD (Fig. 3). This result was within the range of 1 and 1.35 mm measured experimentally by Heuer et al. (2007) under similar boundary conditions. After 4 hours of creep under body weight, the same model predicted a height loss of 1.91 mm (Fig.3), in agreement with the range of values reported by Adams and Hutton (1983).

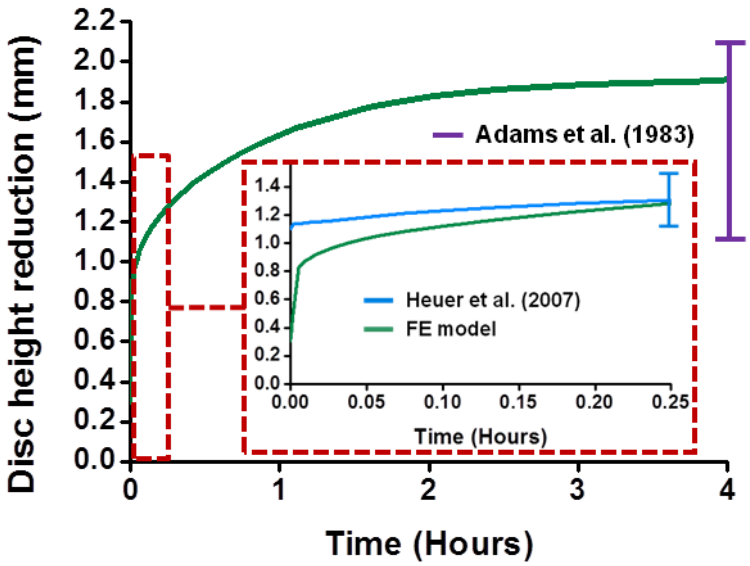

Fig.3 Predictions of disc height reduction performed with the composition-based model under 500 N of compression up to 4 hours (Adams et al. 1983). The zoom area replicates the same conditions as by Heuer et al. (2007) (axial loading of 500N over 900 seconds).

None of the biochemical parameter variations defined, or combinations thereof, affected cell viability. As a result, 100% of cells remained alive during the three days simulated, for all the simulations that resulted from the DOE. In terms of solute distributions, using any (combination of) lower level (i.e. degenerated) parameter value always led to decreased levels of oxygen and glucose and increased levels of lactate. Also, DOE results showed that the biochemical composition parameter that affected most the transport of all disc solutes, in a particular tissue region, was the local initial water content. In terms of oxygen reduction, the NP centre was the most affected region with a standardized effect of 206, followed by the anterior AF with 87 and finally the posterior AF with 83 (Fig.4a). Similar results were obtained for the increase of lactate; however, standardized effects were lower than for the oxygen (Fig. 4). In terms of glucose, the most affected zone was the anterior AF with a standardized effect of 455, followed by the posterior AF with 218 and the NP centre with 215 (Fig. 4c).

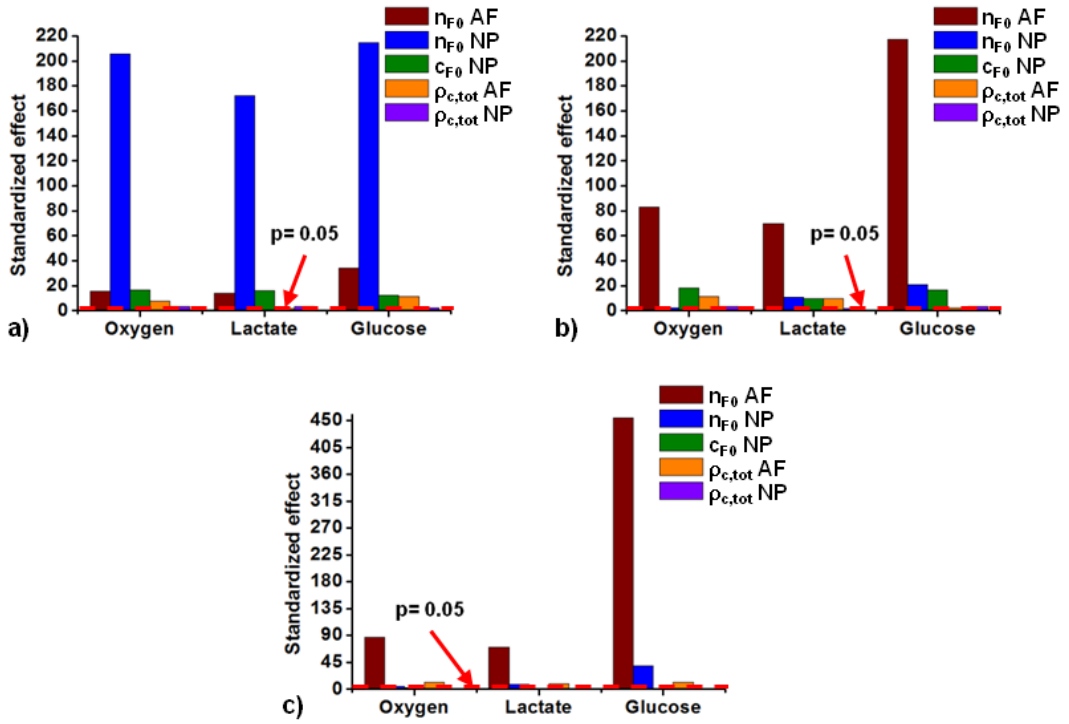

Fig.4 Standardized effect of disc composition parameters variation from grade I to grade III, after 3 days of simulation, on oxygen, lactate and glucose concentrations at: a) NP centre, b) posterior AF and c) anterior AF (Dashed horizontal line is the threshold of significance).

Analysing the solute distributions along the mid-sagittal plane after 3 days, the 16 models created led to a reduced number of groups of results in terms of regional solute concentration (Fig. 5). In the AF, four groups were unequivocally defined (Fig. 5a) according to different combinations of initial water contents in the different IVD subtissues, e.g. per order of decreasing glucose concentrations:

- Group 1: n_{F0} AF and n_{F0} NP representative of grade I
- Group 2: n_{F0} AF representative of grade I and n_{F0} NP representative of grade III
- Group 3: n_{F0} AF representative of grade III and n_{F0} NP representative of grade I
- Group 4: n_{F0} AF and n_{F0} NP representative of grade III

In the NP, two groups of results were identified, as illustrated in Fig. 5b in terms of evolution of the oxygen content over 3 days at the centre of the tissue. The group with high oxygen concentration corresponded to simulations with a NP initial water content representative of grade I, i.e. simulations from the Groups 1 and 3 defined

above. In contrast, the group with lower oxygen concentrations gathered the simulation results with NP initial water content representative of grade III (Groups 2 and 4).

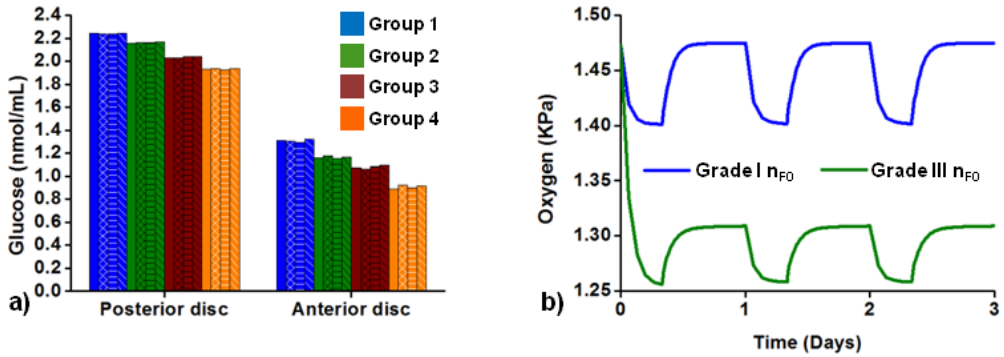

Fig.5 Effect of initial water content (n_{F0}) variations on IVD solute concentrations: a) glucose at the sagittal plane (day 3). The figure shows the groups of results formed according to the initial water contents of the subtissues; group 1: both n_{F0} AF and n_{F0} NP of grade I, group 2: n_{F0} AF of grade I and n_{F0} NP of grade III, group 3: n_{F0} AF of grade III and n_{F0} NP of grade I and group 4: both n_{F0} AF and n_{F0} NP of grade III and b) oxygen at NP centre along three days of simulation. Two groups of results are identified; one with high oxygen content corresponding to simulations with n_{F0} NP of grade I and another group with lower oxygen content corresponding to the results with n_{F0} NP of grade III.

In addition to the direct effects of local composition changes, the ANOVA results also showed that the glucose content in the anterior AF was strongly influenced by the initial water content in the NP (Fig. 6a). However in the posterior AF, the glucose distribution was significantly affected by both the initial water content and the fixed charge density of the NP, and the effect of the local collagen was relatively limited (Fig. 6b).

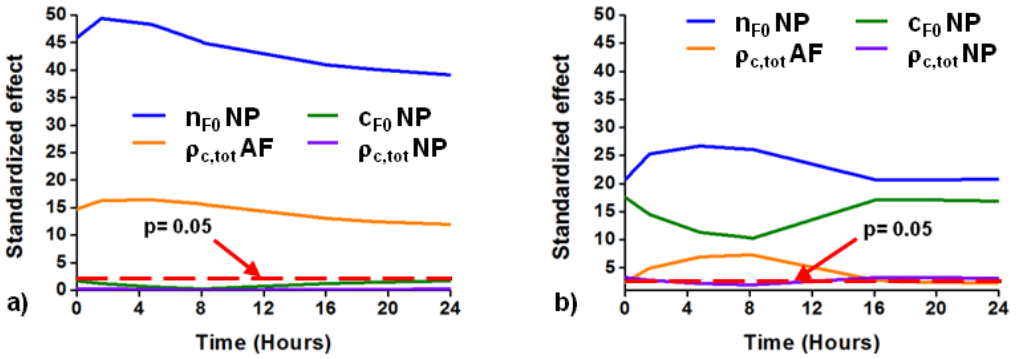

Fig.6 Evolution of the effect of composition parameter variation of the nucleus (n_{F0} NP, c_{F0} NP and $\rho_{c,tot}$ NP) and annulus ($\rho_{c,tot}$ AF) on glucose concentration during a day at: a) the anterior AF and b) the posterior AF. (Dashed horizontal line is the threshold of significance)

All the biochemical changes simulated in this study affected the diurnal height loss after three days. Both at the NP centre and in the posterior AF, the initial fixed charge density of the NP was the parameter that influenced the most the disc height (Fig. 7). For the anterior AF, the AF initial water content was the most relevant parameter followed by the initial fixed charged density of the NP.

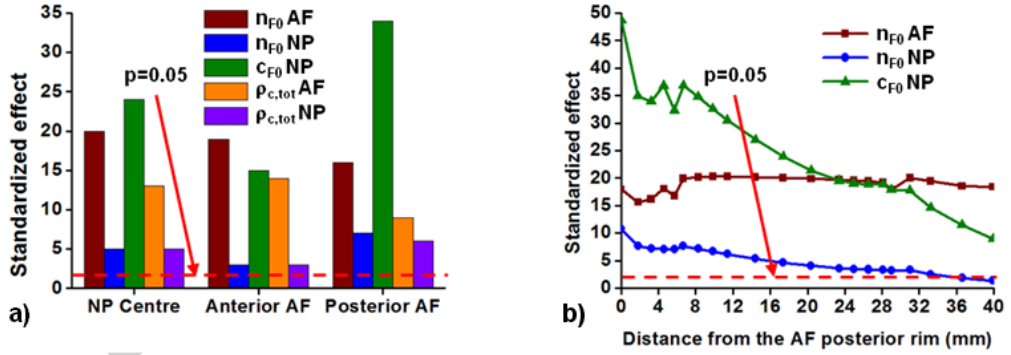

Fig.7 Effect of disc composition parameters (annulus initial water content (n_{F0} AF), annulus collagen content ($\rho_{c,tot}$ AF), nucleus initial water content (n_{F0} NP), nucleus initial fixed charge density (c_{F0} NP), and nucleus collagen content ($\rho_{c,tot}$ NP)) variation on daily disc height: a) after 3 days simulated and b) at the sagittal plane (day 3). (Dashed horizontal line is the threshold of significance)

4. Discussion

The osmo-poroviscoelastic formdulation used in this study was duly verified against thermodynamical consistency (Huyghe et al. 2009). At the tissue level, the model was also validated, with parameter values that represented healthy tissues (Schroeder et al. 2007). In terms of organ validation, the amount of creep measurements available in the literature is limited. In the report of their experimental study, Adams and Hutton (1983) mentioned that the compressive boundary load used corresponded to the body weight, but they did not give any specific value. As such, we took a generic value of 500 N of compressive load (Wilke et al. 1999) in order to replicate their creep study. Assuming that this approximation is acceptable, our results showed that the our healthy model extrapolated reasonably up to 4 hours the simulated behaviour for 15 minutes creep, validated against the measurements reported by Heuer et al. (2007).

Regarding the validity of the degenerated models, our study did not aim to simulate a degenerated disc, but aimed to identify those composition changes that might affect the nutrition of the cells along degeneration, based on biochemically measured quantities. Hence, the variations of phenomenological tissue model parameters such as the stiffness moduli and the permeability were not taken into account. This approximation allowed us focusing our design of experiments on the composition, and was supported by a previous sensitivity analysis reported by Malandrino et al. (2011): by using a similar mechano-transport model, the authors showed that the porosity and the osmotic pressure were the osmo-poromechanical parameters that mostly affected the nutrient transport, being the effect of the stiffness and the permeability parameters negligible. In order to prepare the present study, we have confirmed this outcome through a previous sensitivity analysis that included α and G_m, according to Eqs 7, and 3, respectively (results not shown). Hence, our exploration of the effect of composition changes on the transport of nutrients effectively targeted those tissue model components, i.e. the porosity and the osmotic pressure, most relevant to the metabolic transport calculations.

In our simulations, solute contents were always decreased with degenerative composition changes, but the minimum glucose and pH values were 0.76 nmol/mL and 6.90 respectively, which did not exceed the critical values to see cell death (Horner and Urban 2001). Accordingly, cell viability remained 100% for all the runs performed

during the three days simulated. Glucose and pH thresholds used for cell viability came from in vitro experiments (Horner and Urban 2001). It is difficult to know whether these thresholds are valid in vivo, since no related investigations have been reported so far. However, these criteria have been already used in many numerical studies that have explored the possible role of nutrition in disc degeneration. Malandrino et al. (2014a) used a 3D mechano-transport model to study the mechanical effects on cell viability via transport variations, depending on simulated CEP calcification, AF and NP tissue degeneration, and disc height reduction. Though their tissue constitutive modelling was different from ours, their results supported our findings that moderate AF and NP degeneration only is unlikely to lead to critical glucose levels under physiological load magnitudes and for generic disc geometries. Moreover, the calculations of Malandrino et al. (2014) suggested that simulating CEP calcification (50%) was necessary in order to predict cell death, the latter occurring because of an increased lack of glucose in the inner AF. These results were qualitatively similar to those achieved by Zhu et al. (2012) with a slightly different cell viability function, in which pH was not an explicit trigger of cell death and where cell death rate (i.e. α_{gluc} in Eq. 18) was a nonlinear function of the current glucose concentration. In all these studies, the experiment-based critical glucose concentration of 0.5 mM was the most important assumption for cell death predictions, and all results suggested that nutrition-induced cell death might not be linked to AF and NP degeneration. While our simulations used a similar assumption, and led to a similar outcome, our model allowed a refined control of the specific degeneration changes that may alter cell nutrition in the different tissue.

Supporting to our results, several simulation reports pointed out that the glucose concentration in inner AF is easily affected by any simulated degenerative change (Galbusera et al. 2011; Zhu et al. 2012; Malandrino et al. 2014a). This phenomenon was largely attributed to the strong local consolidation of the TZ regions, due to the lateral pressure exerted on the fibre-reinforced AF by the lateral expansion of the NP under mechanical loads (Ruiz et al. 2013). Among the different mechanotransport - cell viability studies published, our full 3D simulations can be compared directly to the work reported by (Malandrino et al. 2011; 2014a), with the same model geometry. Whilst using a porohyperelastic constitutive model with a fixed osmotic pressure in the NP, these authors always identified the inner anterior AF as the disc region where glucose concentration was mostly reduced. In contrast, we predicted that the cumulated

effect of water and proteoglycan loss within the NP was particularly critical to the availability of glucose in the posterior AF. Interestingly, this issue seemed to arise from the particularly high impact of NP proteoglycan loss on disc height reduction and increased tissue consolidation in the TZ of the posterior AF area. Acknowledging that limited glucose can trigger inflammatory and catabolic responses by disc cells (Neidlinger-Wilke et al. 2012), we may infer that early NP degeneration might contribute to weaken biochemically the posterior AF due to local nutrition issues. Confirmation of this possible non-mechanical weakening would require, however, experimental data about disc cell catabolic activity for different glucose contents between 0.5 and 5 mM.

The composition-based model reproduced the expected disc height reduction under compression changes due to ECM degeneration, i.e. but we did not consider permanent disc height loss. Such a consideration could have modified slightly the computed influence of the diffusion distances (Galbusera et al. 2011; Malandrino et al. 2011). However, this issue is not expected to have a major impact on the current study, since the influence of tissue consolidation is probably predominant, for our particular disc model geometry, as suggested by Malandrino et al. (2011) and further discussed in the next paragraph. Endplate sclerosis was not considered either. Whereas Zhang et al. (2008) considered that this condition rarely appears in grade III discs, Benneker et al. (2005) reported that sclerosis in grade III discs is frequently found. As mentioned earlier, several authors of numerical studies have simulated CEP sclerosis, but the way to do it is not clear, especially for a specific grade, and exploring such simulation hypothesis is beyond the scope of this paper.

Overall, the initial water content is the parameter of disc composition that affected most the transport of solute at the end of the three days simulated. The most affected solute was glucose, especially in the anterior AF. This trend did not change when an ANOVA was performed at the end of each simulated day. The predominant influence of water content is supported by earlier sensitivity studies where a decrease in porosity was reported to affect the transport of oxygen and lactate, more than any other poromechanical parameters did (Malandrino et al. 2011). Simulated composition changes led to disc height reductions in the mechanically loaded disc models, which reduced the effective diffusion distances. However, our results revealed that without any

initial disc height reduction in an unconsolidated state, the possible benefits of the mechanically induced height reduction for diffusion are largely countered by increased tissue consolidation, i.e. decreased current porosity. A similar outcome was suggested by a parameterization of the porosity and diffusion coefficients proposed by Galbusera et al. (2011).

We should, however, recall that our diffusion coefficients were porosity-dependent according to the use of the Mackie-Meares diffusivity law (Eq. 19). This law has been extensively used for several studies on cartilage and intervertebral disc (Maroudas 1968; Frank et al. 1990; Lanir et al. 1998), and seems physically reasonable especially due to likely constrictivity effects (Holzer et al. 2013). Yet, recent measurements showed that the model of Mackie and Meares could slightly underestimate experimental diffusivities (Gu et al. 2004). However, these measurements were performed in agarose gels and not in extracted tissues. Other strain-dependent diffusivity laws have been proposed (Zhu et al. 2012), and how they influence predictions in comparison to the Mackie and Meares law would have to be assessed. Meanwhile, because of the lack of robust experimental studies on disc tissues diffusivities in vitro or in vivo, exploiting the Mackie-Meares model stands for a pragmatic and physically sound approach.

Eq. (1) assumes that the solid phase of the matrix is incompressible for all disc tissues, which implies that the volumetric changes of the poroelastic continuum are due to the gain or loss of water when the tissue deforms. Should the solid phase be compressible, our calculations would overestimate the effects of the volumetric deformations on the diffusion of solutes in the compressed tissue regions. Furthermore, considering solid phase compressibility would modify the relation between diffusion distance and porosity changes, and the positive effect of diffusion distance reductions could become relatively stronger under simulated compression. Yet, it is worth to mention that the solid phase of the NP and AF matrices are rich in proteoglycans: the latter can represent up 85% of the solid phase in the NP (Urban and Roberts 2003). Hence, the steric and electric repulsion forces in and between the glycosaminoglycan aggregates at the nanoscale (Dean et al. 2006; Han et al. 2007), might favour incompressibility of proteoglycan-rich phases at the microscale. Also, the swelling pressure generated by the proteoglycan negative fixed charges, pre-tenses the collagen

fibres and increases the volumetric stiffness of the proteoglycan phase. In our simulations, this swelling pressure is a spherical stress tensor that pre-stresses the solid phase. Hence, we implicitly simulate a hydrated and turgid mix of collagen and proteoglycans at the nanoscale that is likely to appear as a nearly incompressible phase at the scale of several tens of microns.

Though no quantitative measurements are available to our knowledge to test the effective compressibility of the modelled solid phase, analogies with articular cartilage exist in terms of composition and multiphysics interactions among tissue constituents. Miller and Morgan (2010) analysed the results of micro and macro compression tests of articular cartilage and found that the micro- and macro-scale poroelastic properties of the tissue were consistent when derived from a formulation based on Eq. (1). This outcome suggested that the collagen-proteoglycan hydrated matrix could be reasonably considered as incompressible at the microscale. At the macroscopic scale, the use of a poromechanical theory similar to ours could reproduce the response of the articular cartilage for a variety of experiments, i.e. confined and unconfined compression, stress relaxation, indentation, swelling (Wilson et al. 2006).

As anticipated earlier, our simulated degenerative changes in the NP may affect the AF nutrition. In the anterior AF, the effect of n_{F0} in the NP was 39 at the end of one simulated day. This standardized effect was higher than the separate effect of each NP parameter on the glucose concentration in the posterior AF, i.e. 21 for n_{F0}, 17 for c_{F0} and 3 for $\rho_{c,tot}$. However, combining the respective effects of all NP parameters at the posterior AF gave a cumulative effect of 41, slightly higher than the global effect of NP alterations on the anterior AF. According to measurements (Iatridis et al. 2007), NP desiccation and proteoglycan depletion would be concomitant in mildly to moderately degenerated discs, and our findings suggest that such a situation exposes particularly the posterior AF. According to the hypothesis of possible biochemical AF weakening made earlier, such impact of NP alteration on the AF may contribute to explain mechanistically why radial tears in the posterior AF mostly appear in a moderately to severely discs (Osti et al. 1992). Interestingly, calculations indicated that NP dehydration alone affected both the posterior and anterior AF. Here, it becomes worth to mention the possible effect of any early loss of CEP functionality that might contribute to reduce the NP water content by altering the balance of water in-flow and out-flow

along daily loading (Ayotte et al. 2001). Hence, assuming that early NP dehydration is possible, our simulations raise the question whether nutrition issues could play role in the occurrence of circumferential tears, already present in both the anterior and posterior AF of normal to moderately degenerated discs (Osti et al. 1992).

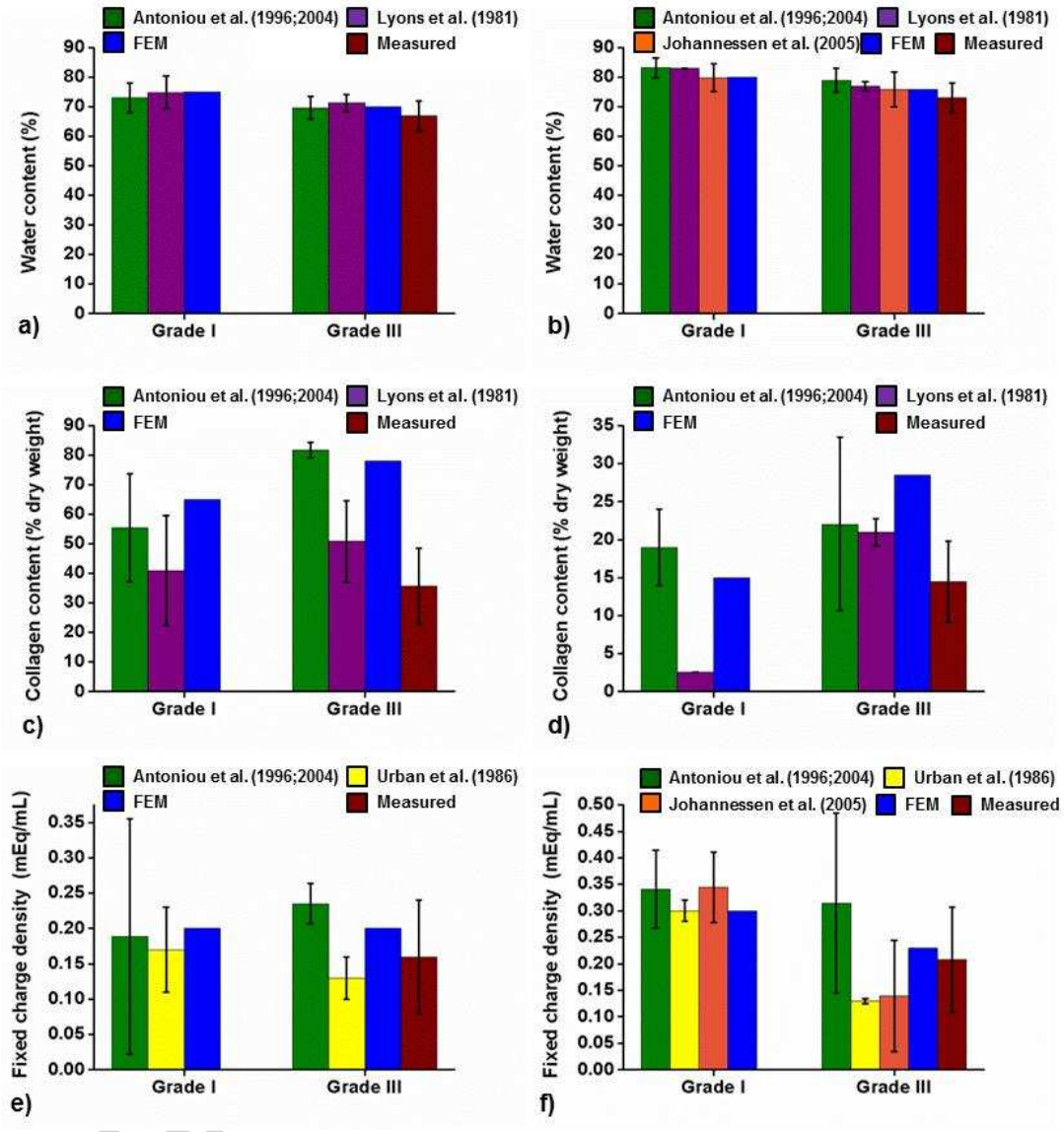

Fig.8 Comparative composition parameters for grade I and grade III discs: a) AF water content (%), b) NP water content (%), c) AF collagen content (% dry weight), d) NP collagen (% dry weight), e) AF fixed charge density (mEq/mL), and f) NP fixed charge density (mEq/mL). Literature data referred to grade III IVD on the Thompson scale (Lyons et al. 1981; Urban and Holm 1986; Antoniou et al. 1996; 2004; Johannessen and Elliott 2005), while in-house measurements referred to grade III IVD on the Pfirrmann scale (Dao et al. 2014).

Fig. 8 shows the mean composition parameters used in this study, in comparison to individual measurements reported in the literature. For the degenerated discs, literature data referred to grade III IVDs on the Thompson scale, which is different from the MRI-based Pfirrmann scale usually used in clinics. In-house biochemical assessments of tissue samples from seven human discs previously graded as grade III on the Pfirrmann scale (Dao et al. 2014) revealed that the water content and fixed charge density used in the model represented mildly to moderately degenerated discs, according to common clinical evaluations (Fig. 8a,b,e,f). As for the collagen content, the value used in the model seems more similar to an advance grade III/early grade IV disc on the Pfirrmann scale (Fig. 8c,d). However, our results showed that changes in the collagen content did not affect the solute concentrations, and only slightly affected the disc height reduction.

This study has the following limitations: first, the three days chosen for the simulations might not be enough for reaching a steady-state for a cell viability study; although we found that a steady-state convergence of two days was enough to observe cell death with a calcified CEP (data not shown) (Malandrino et al. 2014a). Second, we did not simulate dynamic load variations around the mean load value chosen for day activity. Although these loads might limit the loss of water (Schmidt et al. 2010) and could favour the transport of nutrients (Zhu et al. 2012), simulating dynamic loads would have increased the computational cost, and earlier studies (Zhu et al. 2012) suggest that it would not have changed our interpretations. Third, multiaxial loads were not considered in this study. Nevertheless, under external axial compression, most of disc regions are subjected to compression. For the regions that present combined tension-compression, it has been reported that tension-compression nonlinearities affect the estimation of interstitial velocities (Huang et al. 2001; Huang et al. 2003), and have little effect on the transport of small solutes, e.g. glucose and oxygen (Huang and Gu 2007). As such, our mechano-transport predictions would not be affected by not considering such nonlinearities. Fourth, we did not consider any local variations in proteoglycan concentration and total amount of collagen within each modelled tissue. Though such a variation could have better informed the suggested sensitivity of the posterior AF in relation to the anterior AF, we have based our model on specific degeneration-specific composition measurements, made available for this study. Fifth, we did not consider the limitation of Eq. 3 to capture the hysteresis presented by

cartilaginous tissues. The Eq. 3 represents the elastic response of the solid phase and it does not incorporate any term for energy dissipation. Effects of Boltzmann superposition principle are expected to appear from the viscoelastic collagen fibres. However, experiments support the idea that energy dissipation in cartilage matrix is controlled by the fluid flows, captured by poroelastic simulations (Han et al. 2011). As such, integration of Eq. 3 into Eq. 1 is expected to give the capability to represent the NP response to cyclic loads. The predominance of poromechanical time effects in disc tissues was supported by experimental tests on IVD specimens (Costi et al. 2008). However, no direct validation of our tissue models was reported for cyclic loads. Finally, the effect of other important factors related to disc nutrition, e.g. inflammatory factors (Lotz and Ulrich 2006) was not considered, while necessary to assess whether the local nutrient deprivation calculated can weaken the tissues.

5. Conclusions

A composition-based model coupled to a transport-cell viability model was presented as tool to explore the influence of measured ECM changes on disc nutrition and cell viability. This study suggests that small degenerative ECM changes may produce significant solutes alterations. While these changes between grade I and grade III degeneration did not seem relevant to nutrition-related cell viability, they allowed identifying possible mechanisms related to known AF alterations along degeneration. The computational approach developed provides a powerful tool to achieve improved understanding of disc degenerative mechanisms. In particular, our results suggest that the biological and tissue/disc structure changes, able to provoke NP dehydration independently on the further proteoglycan depletion, should be tackled, in order to explore the pathogenesis of the disc in a more integrated way. Obviously, the effect of other important factors related to disc nutrition, e.g. inflammatory factors (Lotz and Ulrich 2006) would be necessary. Our simulations provide, however, a robust framework for such kind of development. The presented model could also be highly relevant to address the challenge of achieving designs of biomimetic IVD implants or scaffold materials that ensure proper mechanical/multiphysics responses in disc regenerative therapies (Noailly et al. 2014).

Acknowledgements

Financial funding from the European Commission (My SPINE-269909) and the Agència de Gestió d'Ajuts Universitaris i de Recerca (AGAUR-2012BE100979) are acknowledged.

References

Adams, M.A., Hutton, W.C., 1983. The effect of posture on fluid content of lumbar intervertebral discs. Spine 8(6), 665-671.

Antoniou, J., Steffen, T., Nelson, F., Winterbottom, N., Hollander, A.P., Poole, R.A., Aebi, M., Alini, M., 1996. The human lumbar intervertebral disc: evidence for changes in the biosynthesis and denaturation of the extracellular matrix with growth, maturation, ageing, and degeneration. J. Clin. Invest. 98(4), 996-1003.

Antoniou, J., Demers, C. N., Beaudoin, G., Goswami, T., Mwale, F., Aebi, M., Alini, M., 2004. Apparent diffusion coefficient of intervertebral discs related to matrix composition and integrity. Magn Reson Imaging, 22(7), 963-972.

Ayotte, D.C., Ito, K., Tepic, S., 2001. Direction-dependent resistance to flow in the endplate of the intervertebral disc: an ex vivo study. J. Orthop. Res. 19, 1073-1077.

Battié, M.C., Videman, T., Levalahti, E., Gill, K., Kaprio, J., 2007. Heritability of low back pain and the role of disc degeneration. Pain 133, 272-280.

Benneker, L., Heini, P., Anderson, S., Alini, M., Ito, K., 2005. Correlation of radiographic and MRI parameters to morphological and biochemical assessment of intervertebral disc degeneration. Eur. Spine J. 14, 27-35.

Bibby, S.R., Jones, D.A., Ripley, R.M., Urban, J.P., 2005. Metabolism of the intervertebral disc: effects of low levels of oxygen, glucose, and pH on rates of energy metabolism of bovine nucleus pulposus cells. Spine 30, 487-496.

Costi, J.J., Stokes, I.A., Gardner-Morse, M.G., Iatridis, J.C., 2008. Frequency-dependent behaviour of the intervertebral disc in response to each of six degree of freedom dynamic loading: Solid phase and Fluid phase contributions. Spine 33(16), 1731-1738.

Dao, T.T., van Rijsbergen, M., Pouletaut, P., Charleux, F., Ito, K., Ho Ba Tho, M.C., 2014. In vitro Assessment of Micro-structural Properties of Intervertebral Disc using 1.5T Magnetic Resonance T2 and ADC Mappings. In: 7th World Congress of Biomechanics, July 6-11, 2014, Boston, Massachusetts, USA.

Dean, D., Han, L., Grodzinsky, A.J., Ortiz, C., 2006. Compressive nanomechanics of opposing aggrecan macromolecules. J Biomech. 39(14), 2555-2565.

Farndale, R.W., Buttle, D.J., Barrett, A. J., 1986. Improved quantitation and discimination of sulphated glycosaminoglycans by use of dimethylmethylene blue. Biochim. Biophy. Acta. 883, 173-177.

Frank, E.H., Grodzinsky, A.J., Phillips, S.L., Grimshaw, P.E., 1990. Physicochemical and Bioelectrical Determinants of Cartilage Material Properties. Biomech. Diarthrodial. Joints., 261-282.

Galbusera, F., Mietsch, A., Schmidt, H., Wilke, H.J., Neidlinger-Wilke, C., 2011. Effect of intervertebral disc degeneration on disc cell viability: a numerical investigation. Comput. Methods Biomech. Biomed. Engin. 16(3), 328-337.

Gu, W.Y., Yao, H., Vega, A.L., Flagler, D., 2004. Diffusivity of ions in agarose gels and intervertebral disc: effect of porosity. Ann. Biomed. Eng. 32, 1710-1717.

Guilak, F., Ting-Beall, H.P., Baer, A.E., Trickey, W.R., Erickson, G.R., Setton. L.A., 1999. Viscoelastic properties of intervertebral disc cells. Spine 24, 2475-2486.

Han, L., Dean, D., Mao, P., Ortiz, C., Grodzinsky, A.J., 2007. Nanoscale shear deformation mechanisms of opposing cartilage aggrecan macromolecules. Biophys. J. 93(5), L23-L25.

Han, L., Frank, E.H., Greene, J.J., Lee, H.Y., Hung, H.H.K., Grodzinsky, A.J., Ortiz, C., 2011. Time-dependent nanomechanics of cartilage. Biophys. J. 100(7), 1846-1854.

Heuer, F., Schmitt, H., Schmidt, H., Claes, L., Wilke, H.J., 2007. Creep associated changes in intervertebral disc bulging obtained with a laser scanning device. Clin. Biomech. 22, 737-744.

Holzer, L., Wiedenmann, D., Münch, B., Keller, L., Prestat, M., Gasser, Ph., Robertson, I., Grobéty, B., 2013. The influence of constrictivity on the effective transport properties of porous layers in electrolysis and fuel cells. J. Mater. Sci. 48(7), 2934-2952.

Horner, H.A., Urban, J.P., 2001. Effect of nutrient supply on the viability of cells from the nucleus pulposus of the intervertebral disc. Spine 26, 2543-2549.

Huang, C.Y., Mow, V.C., Ateshian, G.A., 2001 The Role of Flow-Independent Viscoelasticity in the Biphasic Tensile and Compressive Responses of Articular Cartilage. J. Biomech. Eng. 123(5), 410-417.

Huang, C.Y., Soltz, M.A., Kopacz, M., Mow, V.C., Ateshian, G.A., 2003. Experimental verification of the roles of intrinsic matrix viscoelasticity and tension-compression nonlinearity in the biphasic response of cartilage. J. Biomech. Eng. 125(1), 84-93.

Huang, C.Y., Gu, W.Y., 2007. Effects of tension-compression nonlinearity on solute transport in charged hydrated fibrous tissues under dynamic unconfined compression. J. Biomech. Eng. 129(3), 423-429.

Huszar, G., Maiocco, J., Naftolin, F., 1980. Monitoring of collagen and collagen fragments in chromatography of protein mixturs. Anal. Biochem. 105(1), 424-429.

Huyghe, J.M., Wilson, W., Malakpoor, K., 2009. On the thermodynamical admissibility of the triphasic theory of charged hydrated tissues. J. Biomech. Eng., 131(4), 245-258.

Iatridis, J., MacLean, J., O'Brien, M., Stokes, I., 2007. Measurements of proteoglycans and water content distribution in human lumbar intervertebral discs. Spine 32(14) 1493-1497.

Johannessen, W., Elliott, D.M., 2005. Effects of degeneration on the biophasic material properties of human nucleus pulposus in confined compression. Spine 30(24), 724-729.

Lanir, Y., Schneiderman, R., Huyghe, J.M., 1998. Partition and diffusion of sodium and chloride ions in soft charged foam: the effect of external salt concentration and mechanical deformation. Tissue Eng. 4(4), 365-379.

Lyons, G., Eisenstein, S.M., Sweet, M.B., 1981. Biochemical changes in intervertebral disc. Biochim. Biophys. Acta 673(4), 443-453.

Lotz, J., Ulrich, J.A., 2006. Innervation, inflammation and hypermobility may characterize pathologic disc degneration: review of animal model data. J. Bone. Joint. Surg. Am. 88(2), 76-82.

Mackie, J., Meares, P., 1955. The diffusion of electrolytes in a cation-exchange resin membrane. Proceedings of the Royal Society of London. Series A, Mathematical and Physical Sciences 232, 498-518.

Malandrino, A., Noailly, J., Lacroix, D., 2011. The Effect of Sustained Compression on Oxygen Metabolic Transport in the Intervertebral Disc Decreases with Degenerative Changes. PLoS Comput Biol 7(8).

Malandrino, A., Noailly, J., Lacroix, D., 2014a. Numerical exploration of the combined effect of nutrient supply, tissue condition and deformation in the intervertebral disc. J. Biomech. 47, 607-762.

Malandrino, A., Pozo, J.M., Castro-Mateo, I., Frangi, A., van Rijsbergen, M., Ito, K., Wilke, H.J., Dao, T.T., Ho Ba Tho, M.C., Noailly, J., 2014b. On the relative relevance of subject-specific geometries and degeneration-specific mechanical properties for the study of cell death in human intervertebral disc models. Front. Bioeng. Biotechnol. 3(5), 1-15.

Maroudas, A., 1968. Physicochemical properties of cartilage in the light of ion exchange theory. Biophys. J. 8(5), 575-595.

Miller, G.J., Morgan, E.F., 2010. Use of microindentation to characterize the mechanical properties of articular cartilage: comparison of biphasic material properties across length scales. Osteoarthr. Cartil. 18(8), 1051-1057.

Narmoneva,D.A.,Wang,J.Y.,Setton,L.A.,1999.Nonuniform swelling-induced residual strains in articular cartilage. J.Biomech.32, 401–408.

Neidlinger-Wilke, C., Mietsch, A., Rinkler, C., Wilke, H.J., Ignatius, A., Urban, J., 2012. Interactions of environmental conditions and mechanical loads have influence on matrix turnover by nucleus pulposus cells. J. Orthop. Res. 30, 112-121.

Noailly, J., Malandrino, A., Galbusera, F., 2014. Computational modelling of spinal implants, in J. Zhongmin (Ed.), Computational Modelling of Biomechanics and

Biotribology in the Musculoskeletal System. Woodhead Publishing Ltd., Cambridge, pp. 447–484.

Osti, O., Vernon-Roberts, B., Moore, R., Fraser, R.D., 1992. Annular tears and disc degeneration in the lumbar spine. J. Bone. Joint. Surg. Br. 74(5), 678-682.

Pfirrmann, C.R.W., Metzdorf, A., Zanetti, M., Hodler, J., Boos, N., 2001. Magnetic resonance classification of lumbar interverterbal disc degeneration. Spine 26, 1873-1878.

Roberts, S., Urban, J.P.G., 2011. Intervertebral discs, in: H. Riihimäki & E. Viikari-Juntura (Eds.), Musculoskeletal system, in: J.M. Stellman (Eds.) Encyclopedia of Occupational Health and Safety. International Labor Organization, Geneva.

Ruiz, C., Noailly, J., Lacroix, D., 2013. Material property discontinuities in intervertebral disc porohyperelastic finite element models generate numerical instabilities due to volumetric strain variations. J. Mech. Behav. Biomed. Mater. 26, 1-10.

Schmidt, H., Shirazi-Adl, A., Galbusera, F., Wilke, H.J., 2010. Response analysis of the lumbar spine during regular daily activities--a finite element analysis. J. Biomech. 43(10), 1849-1856.

Schroeder, Y., Sivan, S., Wilson, W., Merkher, Y., Huyghe, J., Maroudas, A., Baaijens, F.P.T., 2007. Are disc pressure, stress, and osmolarity affected by intra and extrafibrillar fluid exchange?. J. Orthop. Res. 25, 1317-1324.

Setton, L.A., Chen, J., 2004. Cell mechanics and mechanobiology in the intervertebral disc. Spine 29, 2710-2723.

Sivan, S., Merkher, Y., Wachtel, E., Ehrlich, S., Maroudas, A., 2006. Correlation of swelling pressure and intrafibrillar water in young and aged human intervertebral discs. J. Orthopaed. Res. 24(6), 1292-1298.

Thompson, J.P., Pearce, R.H., Schechter, M.T., Adams, M.E., Tsang, I.K.Y., Bishop, P.B., 1990. Preliminary evaluation of a scheme for grading the gross morphology of the human intervertebral disc. Spine. 15(5), 411-415.

Urban, J.P., Maroudas, A., 1979. The measurement of fixed charge density in the intervertebral disc. Biochim. Biophys. Acta 586, 166-178.

Urban, J.P., Holm, S.H., 1986. Intervertebral disc nutrition as related to spinal movements and fusion, in A Hargens ed., Tissue Nutr. Viability: New York, NY, Springer-Verlag, 101-119.

Urban, J.P.G., Roberts, S., 2003. Degeneration of the intervertebral disc. Arthritis Res. Ther. 5(3), 120-130.

Urban, J.P.G., Smith, S., Fairbank, J.C.T., 2004. Nutrition of the intervertebral disc. Spine 29, 2700-2709.

Wilke, H.J., Neef, P., Caimi, M., Hoogland, T., Claes, L.E., 1999. New in vivo measurements of pressures in the intervertebral disc in daily life. Spine 24, 755-762.

Wilson, W., Huyghe, J.M., van Donkelaar, C.C., 2006. A composition-based cartilage model for the assessment of compositional changes during cartilage damage and adaptation. Osteoarthr. Cartil. 14(6), 554-560.

Zhang, Y., Zhao, C., Jiang, L., Chen, X., Dai, L., 2008. Modic changes: a systematic review of the literature. Eur. Spine J. 17, 1289-1299.

Zhu, Q., Jackson, A., Gu, W.Y., 2012. Cell viability in intervertebral disc under various nutritional and dynamic loading conditions: 3d Finite element analysis. J. Biomech. 45, 2769-2777.

Vitae

Carlos Ruiz is a PhD candidate in the group of Biomechanics and Mechanobiology of The Institute for Bioengineering of Catalonia (IBEC), Spain. He got his bachelor degree in Mechanical engineering from The Universidad Nacional Experimental Politécnica "Antonio José de Sucre" (UNEXPO Barquisimeto, Venezuela) and Master degree in Material Science and Engineering from The Technical University of Catalonia (UPC Barcelona, Spain). In January of 2011, Carlos joined to the group of Biomechanics and Mechanobiology of IBEC in order to develop a composition-based IVD finite element model, where nutrient transport, cell metabolism and cellular activity-related tissue maintenance will be simulated.

After obtaining his MSc in Mechanical Engineering at the University of Bologna, Andrea Malandrino worked at the Rizzoli Institute (2006-2007) on the validation of subject-specific finite element bone models. He obtained his PhD in 2012 from the Universitat Politècnica de Catalunya. From 2008 to 2013, Andrea has mainly focused on the intervertebral disc biotransport and mechanobiology through multiscale finite element modelling, as a researcher at the Institute for Bioengineering of Catalonia. He has also explored the microporomechanical characterization of the human vertebral bone. He is currently a Marie Sklodowska-Curie postdoctoral fellow at Massachusetts Institute of Technology.

Marc van Rijsbergen is a PhD candidate in the group of Orthopaedic Biomechanics of the Eindhoven University of Technology, The Netherlands. He got his Master degree in Medical Engineering from Eindhoven University of Technology (TU/e, Eindhoven, the Netherlands). Since September 2011, Marc is part of the Orthopaedic Biomechanics group and has the task to develop a degenerated biochemical based IVD finite element model, based on the individual tissue composition and mechanical behaviour, including cell metabolism and cellular activity-related tissue maintenance both inside the IVD as well as adjacent bone tissue (mechanoregulated tissue adaptation).

Damien Lacroix is Professor of Mechanobiology in the Department of Mechanical Engineering of the University of Sheffield, UK. He has a first degree in Mechanical Engineering from the National Institute of Applied Science (INSA Lyon, France) and a PhD in Biomechanics from Trinity College Dublin. After various post-doc and fellowships in France and Spain, he was Group Leader of Biomechanics and Mechanobiology from 2008 at the Institute of Bioengineering of Catalonia (Spain). Damien joined the University of Sheffield in 2012 when he took a Chair in Biomedical Engineering within the INSIGNEO research institute. His main research activities include virtual physiological human modelling, mechanobiology, tissue engineering, lumbar disc degeneration, implant design, and cell mechanics.

Keita Ito is a professor in Biomedical Engineering at the Eindhoven University of Technology and in Orthopaedics at the University Medical Center Utrecht. He and his group focus on the mechanobiology of degenerative diseases in bone, articular cartilage and intervertebral disc as well as regeneration in these tissues. He holds a PhD in medical engineering and physics from MIT and an MD from Harvard Medical School. He is a board member of ISSLS, the World Council of Biomechanics and the AO Foundation, and serves on the editorial boards of Tissue Eng., J Ortho Res, Eur Spine J, and J Biomech.

Jérôme Noailly began his PhD in 2002 at the Universitat Politècnica de Catalunya (UPC). He explored the mechanical communications within the lumbar spine through finite element modelling, and addressed model approximation and reliability issues. From 2007 to 2011, he was a Marie Sklodowska-Curie postdoctoral fellow, first at the AO Research Institute, and then at the Institute for Bioengineering of Catalonia (IBEC). During this time, he focussed on soft tissue and multiphysics modelling. In 2009, Jérôme received the best PhD thesis award in engineering from the UPC, and in 2012 he became the head of IBEC's group of Biomechanics and Mechanobiology.

Highlights

- Composition-based osmo-poro-hyperelastic lumbar disc models were coupled to a reaction-diffusion model of oxygen, glucose, and lactate, involved in cell nutrition.
- We used a design of experiment to find the composition changes in water, proteoglycan, and collagen that mostly altered disc nutrition.
- Composition degenerative changes always reduced the glucose contents in the discs.
- Tissue dehydration mostly hindered glucose availability throughout the disc.
- Further proteoglycan depletion in the nucleus affected particularly cell nutrition in the posterior annulus due to local consolidation effects.

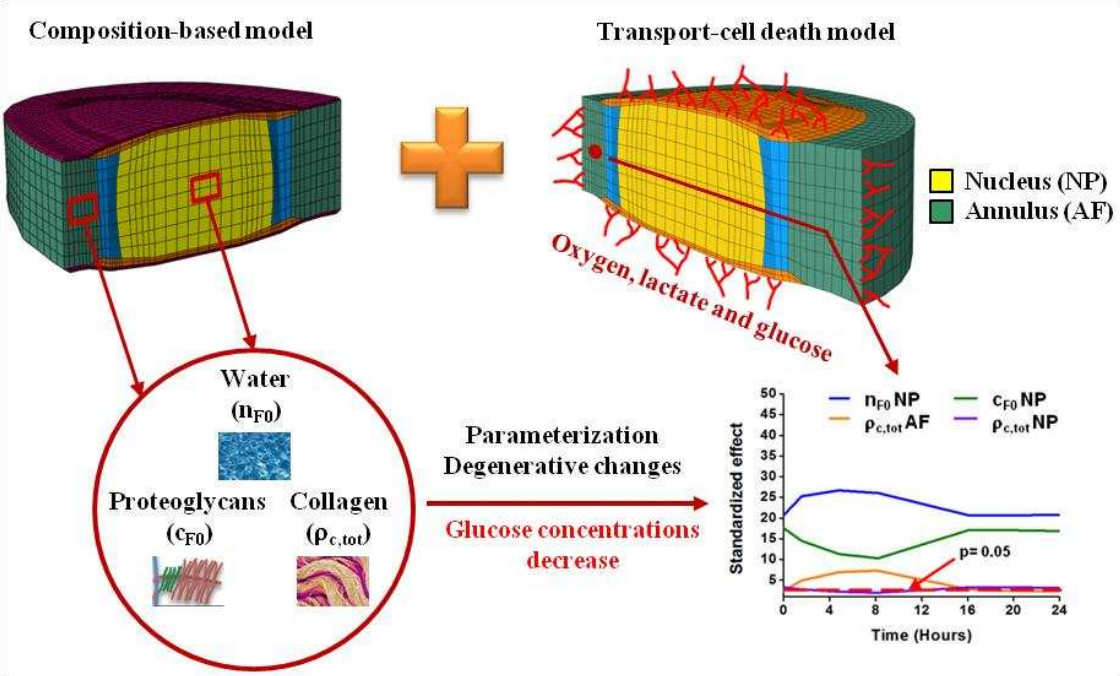

Highlights

- Composition-based osmo-poro-hyperelastic lumbar disc models were coupled to a reaction-diffusion model of oxygen, glucose, and lactate, involved in cell nutrition.
- We used a design of experiment to find the composition changes in water, proteoglycan, and collagen that mostly altered disc nutrition.
- Composition degenerative changes always reduced the glucose contents in the discs.
- Tissue dehydration mostly hindered glucose availability throughout the disc.
- Further proteoglycan depletion in the nucleus affected particularly cell nutrition in the posterior annulus due to local consolidation effects.